

# Ship Detection Requirements Analysis for Different Sea States: Validation on Real SAR Data

Jaime Martín-de-Nicolás, David Mata-Moya, Nerea del-Rey-Maestre, Pedro Gómez-del-Hoyo, María-Pilar Jarabo-Amores

**Abstract**—Ship detection is nowadays quite an important issue in tasks related to sea traffic control, fishery management and ship search and rescue. Although it has traditionally been carried out by patrol ships or aircrafts, coverage and weather conditions and sea state can become a problem. Synthetic aperture radars can surpass these coverage limitations and work under any climatological condition. A fast CFAR ship detector based on a robust statistical modeling of sea clutter with respect to sea states in SAR images is used. In this paper, the minimum SNR required to obtain a given detection probability with a given false alarm rate for any sea state is determined. A Gaussian target model using real SAR data is considered. Results show that SNR does not depend heavily on the class considered. Provided there is some variation in the backscattering of targets in SAR imagery, the detection probability is limited and a post-processing stage based on morphology would be suitable.

**Keywords**—SAR, generalized gamma distribution, detection curves, radar detection.

## I. INTRODUCTION

**S**YNTHETIC Aperture Radars (SARs) are capable of generating high-resolution remote-sensing images of the electromagnetic energy backscattered by the Earth surface. SAR systems are installed aboard mobile platforms, such as spacecrafts, using the platform movement to obtain a larger synthetic antenna and improve azimuth resolution. As SAR systems can be used regardless of meteorological conditions, can operate at night due to their illumination properties [1], [2], they have become powerful tools to map terrain and sea surfaces and to detect and classify point and extended targets. Some applications deal with the maritime traffic or natural disasters monitoring. The fact that the origin and properties of SAR images are different from optical ones makes necessary the development of new signal processing algorithms and/or the adaptation of conventional ones to allow the automatic interpretation of contained information.

One of the problems to solve in SAR imagery is to reduce the speckle noise. Speckle noise is always present in SAR images. This noise is due to the coherent sum of many elementary scatterers in each resolution cell and gives a grainy appearance to images, which makes detection and classification tasks more complex [1]. The presence of

Jaime Martín-de-Nicolás, David Mata-Moya, Nerea del-Rey-Maestre, Pedro Gómez-del-Hoyo, and María-Pilar Jarabo-Amores are with the Signal Theory and Communications Department of the University of Alcalá, Alcalá de Henares, Madrid CP 28805, Spain (e-mail: jaime.martinn@uah.es, david.mata@uah.es, nerea.rey@uah.es, pedrojose.gomez@uah.es, mpilar.jarabo@uah.es).

This work has been supported by the Spanish “Ministerio de Economía y Competitividad”, under projects TEC2012-38701 and TEC2015-71148-R, and by the University of Alcalá, under project CCG2015/EXP070.

speckle noise makes difficult the statistical modeling of the data, which has become a crucial task to address for SAR interpretation (such as pattern recognition, coastline estimation or ship detection). In addition, the dispersive characteristics of the sea surface, affected by many different meteorological phenomena, make the image analysis to be quite tough. This variability demonstrates the importance of developing adaptive techniques associated to the different areas in a SAR image.

The conventional ship detector, which is an important problem in sea traffic control, fishery management and ship search and rescue, is usually based on adaptive threshold algorithms using Constant False Alarm Rate (CFAR) techniques. The performance is highly dependent on the knowledge of the clutter statistics. In [3]–[8] statistical clutter models for terrain and marine SAR data were proposed. In [9], it was concluded that the best model, among several that were studied, was the Generalized Gamma model, which will be used in this paper as the sea clutter model in a ship detection application. This model showed its versatility as it adapted extremely well to several sea states. The goal of this paper will be the analysis of those sea states in terms of SNR (Signal-to-Noise Ratio), and how this value affects the  $P_D$  (Probability of detection) and the  $P_{FA}$  (Probability of false alarm) in a ship detection application using real SAR data. The considered detector is based on the Neyman-Pearson (NP) criterion [10], which maximizes the  $P_D$  maintaining the  $P_{FA}$  equal or lower to a given value, using Generalized Gamma clutter model and Gaussian target model. If  $\mathbf{z}$  is the observation vector and  $f(\mathbf{z}|H_0)$  and  $f(\mathbf{z}|H_1)$  are the detection problem likelihood functions, a possible implementation of the NP detector consists in comparing the Likelihood Ratio (LR),  $\Lambda(\mathbf{z})$ , to a threshold ( $\eta_{lr}$ ) selected according to  $P_{FA}$  requirements, and decide in favor of  $H_1$  when the LR output is higher than the selected threshold (1).

$$\Lambda(\mathbf{z}) = \frac{f(\mathbf{z}|H_1)}{f(\mathbf{z}|H_0)} \underset{H_0}{\underset{H_1}{\gtrless}} \eta_{lr}(P_{FA}) \quad (1)$$

## II. SEA STATE CLASSIFICATION

Using the study carried out in [9], a set 8,100 500x500-pixel patches is considered in order to define the different observed sea states. Five classes were defined with the following properties:

- First class: Sea clutter returns with a linear and very narrow structure that does not respond to wave fields (Figs. 1 (c) and (h)).

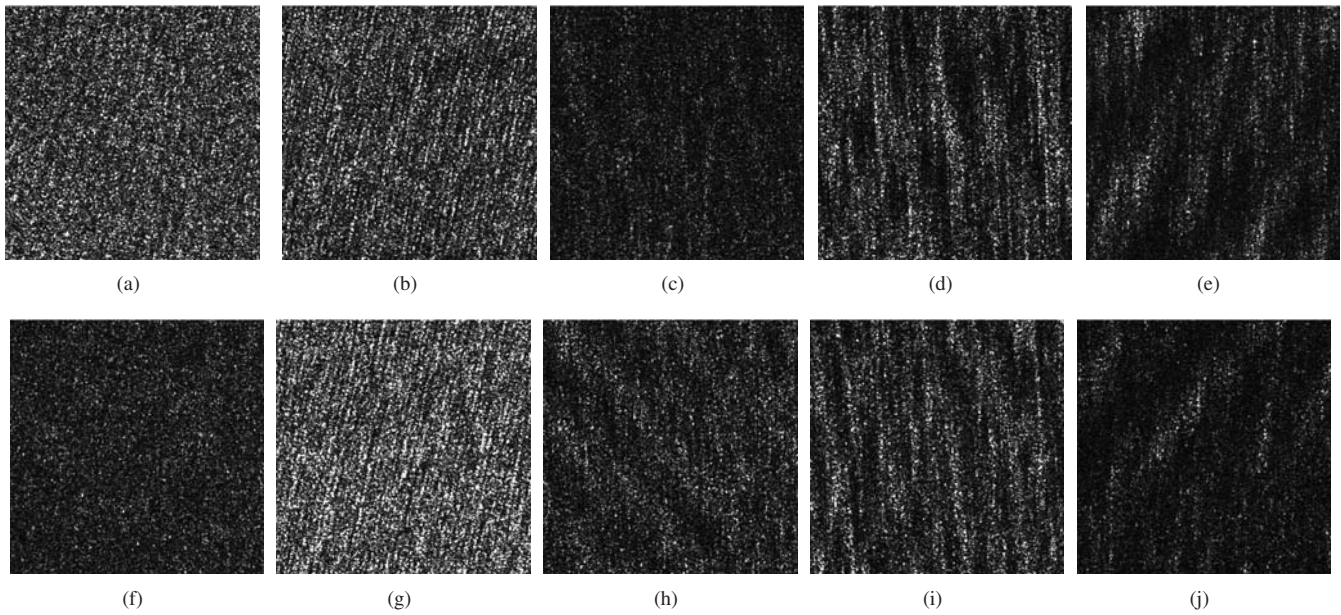


Fig. 1 Examples of  $500 \times 500$ -pixel patches of each class: The five columns correspond to the five classes defined in Section II

- Second class: Sea clutter without a structure visible. The gray level of pixels are distributed without any pattern (Figs. 1 (e) and (j)).
- Third class: Sea clutter echoes with high waves and different wavelengths. As the waves are higher than in the first class, the difference in gray level between the crest and the trough is also higher. Crests tend to be closer to white and troughs closer to black (Figs. 1 (b) and (g)).
- Fourth class: Sea clutter associated to wave fields where crests and troughs are partially defined and they hardly appear to be linear as in first and second classes (Figs. 1 (d) and (i)).
- Fifth class: Sea clutter returns with low to medium height waves and different wavelengths. The gray level of the crest and the trough are both at medium levels (Figs. 1 (a) and (f)).

### III. DETECTOR BASED ON THE GENERALIZED GAMMA CLUTTER MODEL

The detector proposed in [11], a fast block CFAR detector especially suitable for very-high-resolution SAR images, is used in this paper for ship detection. As a first step, the area of interest is divided into equally-sized patches, depending on the resolution and the pixel spacing of the considered image. After this, the brightest pixels of each patch are filtered so that the remaining pixels belong mostly exclusively to the sea surface, and a statistical modeling of the sea clutter is performed. It is widely extended the assumption of a Gaussian model for the sea clutter in this kind of detectors [12]- [14], and had the goal been just the detection of the ship or the definition of an area where the ship is contained, it would have sufficed; however, in the spirit of making the most of the resolution current SAR sensors can achieve, a heavy-tailed distribution is selected, for it models better the SAR sea clutter distribution

[9] and therefore, a better and more accurate ship detection is expected. It is for this reason that the Generalized Gamma distribution is chosen to model the background clutter, whose PDF (Probability Density Function) is as:

$$y = f(x|k, \nu, \sigma) = \frac{|\nu|k^k}{\sigma\Gamma(k)} \left(\frac{x}{\sigma}\right)^{k\nu-1} \cdot \exp\left(-k\left(\frac{x}{\sigma}\right)^\nu\right) \quad (2)$$

where  $k > 0$  is the shape parameter,  $\sigma > 0$  the scale parameter and  $\nu \neq 0$  the power parameter. It can model both amplitude and intensity fluctuations and has several special cases: Rayleigh ( $\nu = 2, k = 1$ ), exponential ( $\nu = 1, k = 1$ ), Nakagami ( $\nu = 2$ ), Gamma ( $\nu = 1$ ), lognormal ( $k \rightarrow \infty$ ) and Weibull ( $k = 1$ ).

With the parameters estimated in every patch, the CDF (Cumulative Distribution Function) of the clutter is modeled and by means of a selected  $P_{FA}$ , a decision threshold inherent to the patch under study is set. Thus, the selection of this threshold is adaptively achieved, providing a good insight into the different states of the sea. What should be remarked about this detector is its ability to detect ships with one-pixel-resolution. Therefore, not only will ships be detected, but they will also be better defined, for information about their size could be provided with more detail, and the variability of ship size will not become an issue. Another important problem in high-resolution SAR imagery is related to the fact that moving targets are unfocused. ISAR techniques have been proposed for focusing ships, extracting dominant scatterers and other features intended for classification purposes. The correct extraction of the information related to the ship is a key issue for improving the performance of these techniques. The detector used in this paper can fulfill this complex requirement.

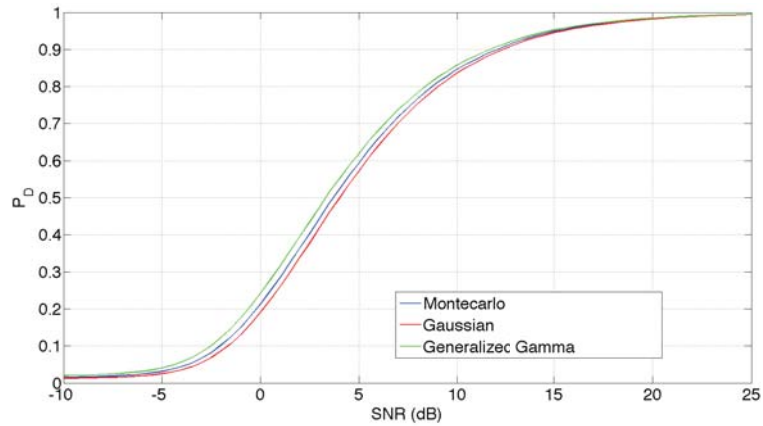


Fig. 2 Relation between the SNR and the  $P_D$  for the first class

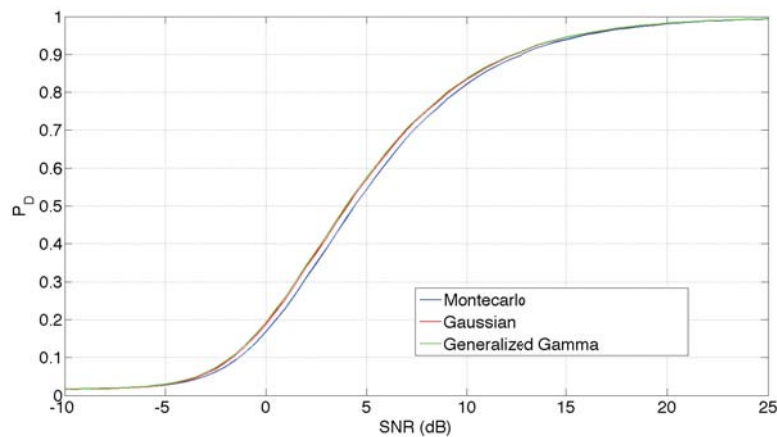


Fig. 3 Relation between the SNR and the  $P_D$  for the second class

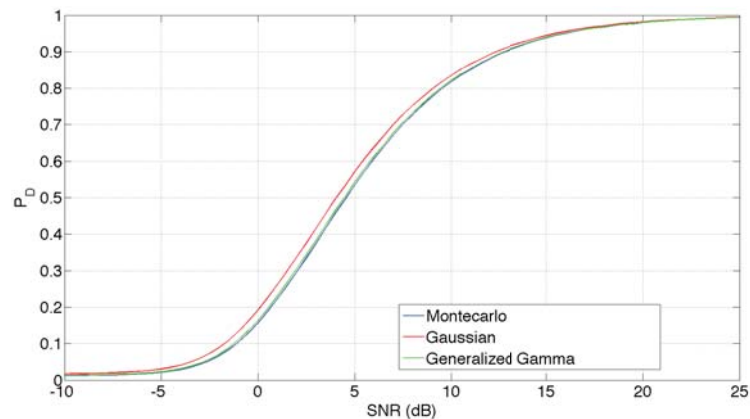


Fig. 4 Relation between the SNR and the  $P_D$  for the third class

#### IV. RESULTS

##### A. SNR Requirements Analysis

In order to define SNR requirements to detect vessels in different sea states, detection curves were analyzed assuming target Gaussian model based on Swerling models [15], [16]. The detection curves show the minimum SNR required to obtain the desired  $P_D$  with a given  $P_{FA}$ . The detection capabilities were estimated using real clutter data of each class defined according to the sea state. Two patches of

500x500 pixels are used, the first one to estimate the threshold associated with the specified  $P_{FA}$ , and the second one to estimate the corresponding  $P_D$  resulting of adding a synthetic Gaussian target with different SNRs.

Empirical results, used as reference ones, were estimated using Montecarlo Simulation.  $P_{FA} = 10^{-2}$ , with an associated estimation error of 0.2% with regard to patch size, was considered to estimate the corresponding threshold. Using the same patches associated with each class, new thresholds

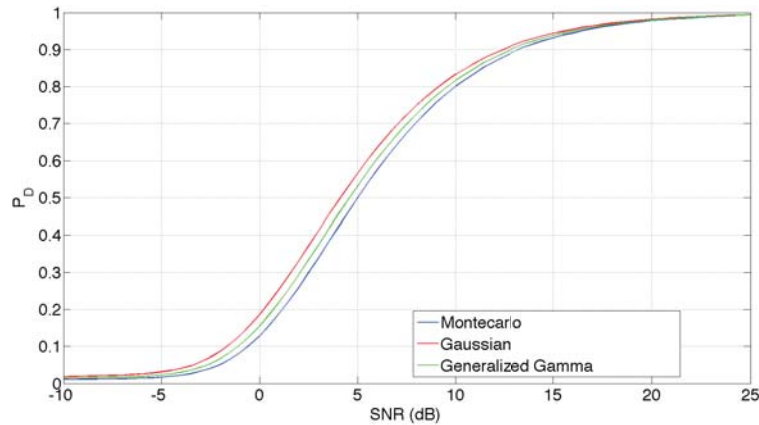


Fig. 5 Relation between the SNR and the  $P_D$  for the fourth class

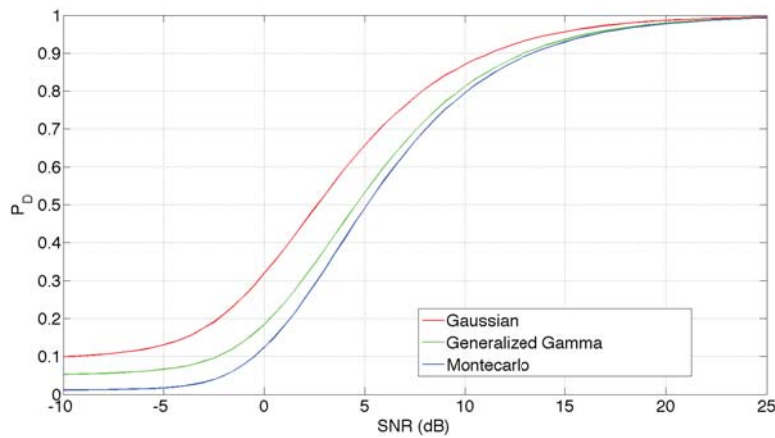


Fig. 6 Relation between the SNR and the  $P_D$  for the fifth class

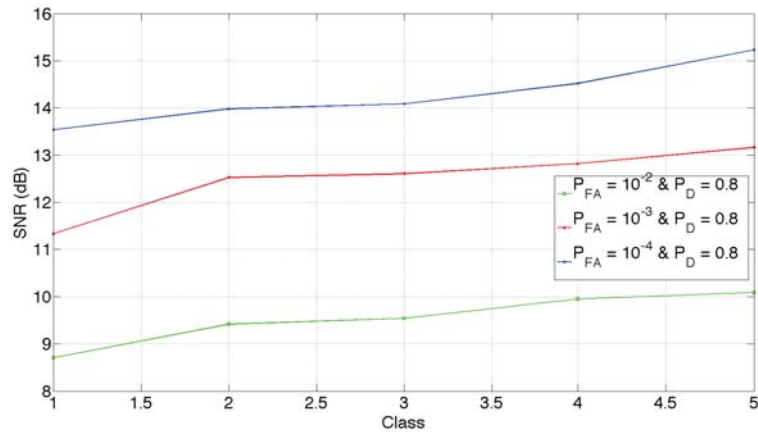


Fig. 7 SNR of the five classes for a fixed  $P_D$  of 80%

Open Science Index, Electronics and Communication Engineering Vol:10, No:11, 2016 publications.waset.org/10005645/pdf

are also determined using statistical parameters estimated assuming Gaussian model, widely used in the literature [12]-[14], and Generalized Gamma model that presents a good results to fit sea clutter in different sea states [9].

The comparative detection curves are presented in Figs. 2-6. As can be seen, the Generalized Gamma model is closer to the Montecarlo simulation in most cases, especially when the sea state is higher, and in those cases where the Gaussian model is closer, the difference between this model and the Generalized

Gamma is not important. Therefore, results confirm that the Generalized Gamma model is expected to perform correctly with every sea state.

Figs. 2-6 provide the SNR requirements for any  $P_D$  and any sea state class. In Fig. 7, the dependence of the minimum SNR needed in order to ensure such a  $P_D \geq 80\%$  on the sea state is detailed. Using the threshold corresponding to an approximation to a Generalized Gamma model for  $P_{FA} = 10^{-2}, 10^{-3}$  and  $10^{-4}$ , it can be observed that the SNR does

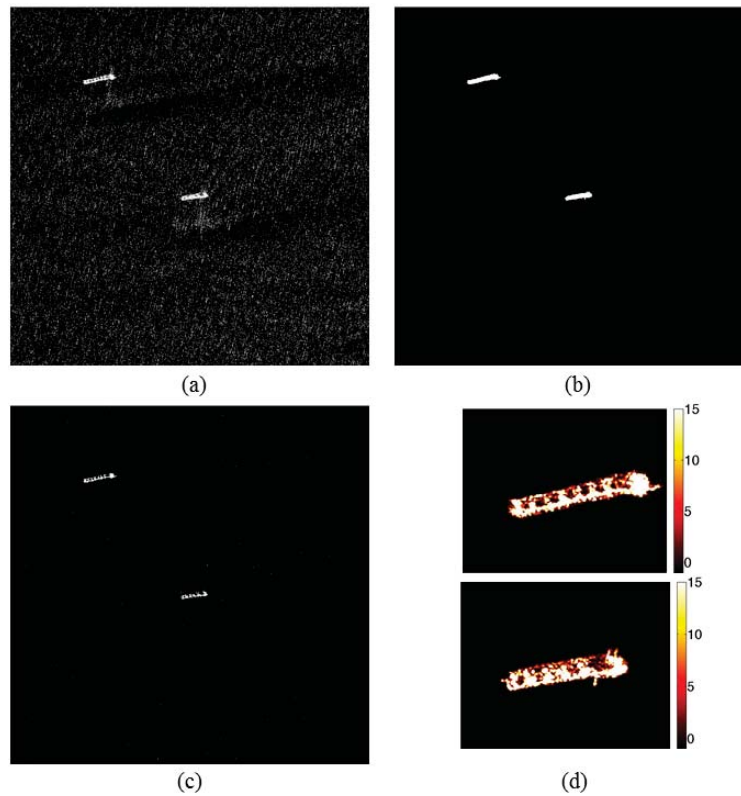


Fig. 8 (a) original SAR image; (b) manually-estimated mask; (c) result of the ship detector based on the Generalized Gamma model; (d) pixel-level SNR of both ships

not depend heavily on the class considered.

### B. Ship Detection

In order to confirm the previous study, a subimage with two ships is selected (Fig. 8 (a)). The image is a GEC/SE stripmap with HH polarization, with both ground range and azimuth resolution of 3m, 1.45 range looks, 1.039 azimuth looks and a size of  $52,400 \times 37,200$  pixels.

First, a manually-estimated mask is attained to serve as a comparison to the result of the proposed detector and so that the  $P_D$  and the  $P_{FA}$  can be accurately estimated. This mask is shown in Fig. 8 (b). The result of the detector based on the Neyman-Pearson criterion presented in Section III for a  $P_{FA}$  equal to  $10^{-4}$ , presented in Fig. 8 (c), shows that although most parts of both ships are detected, some internal areas are not. This is due to their low backscattering, which results in a lower SNR. Therefore, the  $P_D$  attained is pretty low, with a value equal to 48.77%, while the resulting  $P_{FA}$  is equal to  $2.27 \cdot 10^{-4}$ , which is similar to the design requirements. As said before, the explanation to this low  $P_D$  is the difference in intensity of the signal reflected by the ships; in other words, the difference in SNR. As a matter of fact, the SNR values of the pixels within the ships are represented in Fig. 8 (d), and given that the SNR for a  $P_D$  equal to 48.77% is close to 9 dB, it is clear that plenty of those pixels have a SNR well under that threshold, thus being undetectable and requiring a post-processing stage to include the semantic environment.

### V. CONCLUSION

An analysis of the ship requirements in terms of SNR was carried out in this paper, considering five different sea states first defined in a database described in [9], and using real SAR data. Detection curves were analyzed assuming target Gaussian model based on Swerling models and a Generalized Gamma model for the sea clutter. These model were used in a comparison with a Montecarlo simulation and a Gaussian clutter model, which is commonly used.

The analysis of the different sea states showed that the Generalized Gamma model is closer to the Montecarlo simulation in most cases, especially when the sea state is higher, and in those cases where the Gaussian model is closer, the difference between the two models is not significant. SNR requirements for any  $P_D$  and any sea state class was determined and it was observed that the SNR did not depend heavily on the class considered.

Provided there is some variation in the backscattering of targets in SAR imagery, which results in a lower SNR, the detection probability is limited and, although most parts of both ships are detected, some internal areas are not. Therefore, in order to overcome this issue, a post-processing stage based on morphology or semantic information would be desirable.

### REFERENCES

- [1] J. C. Curlander and R. N. McDonough, *Synthetic Aperture Radar: Systems and Signal Processing*. Wiley-Interscience, 1991.
- [2] R. Bamler, "Principles of synthetic aperture radar," *Surveys in Geophysics*, vol. 21, pp. 147–157, 2000.

- [3] V. Anastassopoulos, G. A. Lampropoulos, A. Drosopoulos, and M. Rey, "High resolution radar clutter statistics," *IEEE Transactions on Aerospace and Electronic Systems*, vol. 35, no. 1, pp. 43–60, January 1999.
- [4] J. Carretero-Moya, J. Gismero-Menoyo, A. B. del Campo, and A. Asensio-López, "Statistical analysis of a high-resolution sea-clutter database," *IEEE Transactions on Geoscience and Remote Sensing*, vol. 48, no. 4, pp. 2024–2037, April 2010.
- [5] S. Chitroub, A. Houacine, and B. Sansal, "Statistical characterisation and modelling of sar images," *Elsevier Signal Processing*, vol. 82, no. 1, pp. 66–92, 2002.
- [6] Y. Delignon, R. Garello, and A. Hillion, "Statistical modelling of ocean sar images," *IEE Proceedings on Radar, Sonar and Navigation*, vol. 144, no. 6, pp. 348–354, December 1997.
- [7] G. Gao, "Statistical modeling of sar images: A survey," *Sensors*, vol. 10, pp. 775–795, 2010.
- [8] E. Kuruoglu and J. Zerubia, "Modeling sar images with a generalization of the rayleigh distribution," *IEEE Transactions on Image Processing*, vol. 13, no. 4, pp. 527–533, April 2004.
- [9] J. Martín-de-Nicolas *et al.*, "Statistical Analysis of SAR Sea Clutter for Classification Purposes," *Remote Sensing*, vol. 6, no. 10, pp. 9379–9411, 2014.
- [10] J. Neyman and E. S. Pearson, "On the problem of the most efficient test of statistical hypotheses," *Springer New York*, 1992.
- [11] J. Martín-de-Nicolás *et al.*, "A Non-Parametric CFAR Detector Based on SAR Sea Clutter Statistical Modeling," in *IEEE International Conference on Image Processing*, 2015.
- [12] C. Wang *et al.*, "Ship Detection for High-Resolution SAR Images Based on Feature Analysis," *IEEE Geoscience and Remote Sensing Letters*, vol. 11, no. 1, pp. 119–123, January 2014.
- [13] S. Brusch *et al.*, "Ship Surveillance With TerraSAR-X," *IEEE Transactions on Geoscience and Remote Sensing*, vol. 49, no. 3, pp. 1092–1103, March 2011.
- [14] M. Martorella, F. Berizzi, D. Pastina, and P. Lombardo, "Exploitation of cosmo skymed sar images for maritime traffic surveillance," in *IEEE Radar Conference*, May 2011, pp. 113–117.
- [15] D. Pastina, G. Battistello, and A. Aprile, "Change detection based GMTI on single channel SAR images," in *European Conference on Synthetic Aperture Radar*, 2008.
- [16] C. J. Willis, "Target modelling for SAR image simulation," *SPIE Remote Sensing*, 2014.